ISBN: 978-1-925627-03-9

Positive surge propagation in non-rectangular channels

Urvisha Kiri[1], Xinqian Leng[2], Hubert Chanson[3]

[1]Research student, The University of Queensland, School of Civil Engineering, Brisbane 4072, Australia

[2]Ph.D. Research student, The University of Queensland, School of Civil Engineering, Brisbane 4072, Australia

[3]Professor, The University of Queensland, School of Civil Engineering, Brisbane 4072, Australia
E-mail: h.chanson@uq.edu.au

Abstract

In an open channel, a positive surge is the unsteady flow motion induced by a sudden rise in water elevation, and may include rejection surges in hydro-power canals and surges induced by rapid gate operation. While the literature is focused on surge propagation in rectangular channels, the present investigation considered the upstream propagation of positive surges in an asymmetrical trapezoidal channel. Detailed experiments were performed in a 19 m long 0.7 m wide flume. Unsteady measurements were conducted using acoustic displacement meters and ADV Profiler. A key feature was the three-dimensional unsteady flow motion. This yielded some complicated transient secondary motion and enhanced transverse mixing compared to positive surge propagation in rectangular channels.

1. INTRODUCTION

A positive surge is an unsteady rapidly-varied open channel flow motion, characterised by an increase in water depth (Henderson 1966). It is also called compression wave and hydraulic jump in translation. A wide range of practical applications encompasses rejection surges in hydro-power canals during sudden decrease in power output, surges travelling downstream following a rapid gate opening, tidal bores in estuaries, and tsunami bores (Ponsy and Carbonnell 1966, Cunge 1975, Chanson 2004,2011, Yasuda 2010) (Fig. 1). The surge propagation is associated with intense mixing and sediment upwelling and suspension, as observed in tidal bore affected estuaries (Chanson et al. 2011, Keevil et al. 2015, Furgerot et al. 2016).

To date, most laboratory investigations were conducted in rectangular channels, but for the free-surface measurements of Sandover and Taylor (1962), Benet and Cunge (1971) and Treske (1994) in trapezoidal channels. Herein detailed free-surface and velocity measurements were performed in a large-size facility (19 m long, 0.7 m wide) with an asymmetrical trapezoidal cross-section. The work focused on the unsteady turbulent properties of the three-dimensional flow, to gain some insight into the transverse mixing induced by unsteady secondary motion.

Figure 1 – Tidal bore of the Qiantang River at at Laoyanchang (China) on 23 September 2016.

2. EXPERIMENTAL METHODS AND FACILITIES

2.1. Experimental apparatus and instrumentation

New experiments were conducted in a 19 m long 0.7 m wide tilting flume, previously used by Leng and Chanson (2016,2017) with a rectangular cross-section. The channel bed was modified with the installation of a 1V:5H transverse slope, made out of PVC (Fig. 2). A fast-closing Tainter gate was located at the channel's downstream end and its rapid closure generated a positive surge propagating upstream. Figure 2 presents a dimensioned sketch of the channel cross-section and Figure 3 shows the upstream propagation of positive surges.

The discharge was provided through an upstream intake structure equipped with flow straighteners followed by a three-dimensional convergence and was measured by a magneto flow meter. In steady flows, the water depths were measured using rail mounted pointer gauges and velocity measurements were conducted with a Dwyer® 166 Series Prandtl-Pitot tube (∅ = 3.18 mm). The Prandtl-Pitot tube was calibrated to provide the boundary shear stress with the tube lying on the boundary (Cabonce et al 2017). The unsteady water depths were recorded non-intrusively using a series of acoustic displacement meters Microsonic™ Mic+ located along and above the channel. The acoustic displacement meters (ADMs) were calibrated against the pointer gauge in steady flows. The unsteady velocity measurements were conducted with an acoustic Doppler velocimeter (ADV) Profiler Nortek™ Vectrino II equipped with a three-dimensional down-looking head, located at x = 8.6 m and sampled at 100 Hz. (Note that the physical experiments were conducted in 2017, after a manufacturer's re-calibration of the unit.) The experiments were documented using a digital SLR camera Pentax™ K-3 as well as a digital camera Casio™ Exilim EX-10 with high-speed video capabilities.

2.2. Initial steady flow conditions and experimental program

Steady flow observations were conducted for discharges between 0.0147 m^3/s and 0.1017 m^3/s (Table 1). In Table 1, S_o is the longitudinal bed slope and d_1 is the initial water depth measured along the right sidewall. The open channel flow was at uniform equilibrium along most of the channel and the flow motion was subcritical, albeit transcritical $0.9 < Fr_o < 1$, with $Fr_o = V_1/(g \times A_1/B_1)^{1/2}$ the initial flow Froude number, V_1 the initial flow velocity, A_1 the initial flow cross-section area and B_1 the initial free-surface width. The free-surface was horizontal in the transverse direction. Typical velocity contour plots are shown in Figure 4. Note the different legends between Figures 4A, 4B and 4C. All results showed a faster flow towards the deeper section of the channel.

The boundary shear stress data indicated that the boundary shear stress distribution was not uniform along the wetted perimeter. Significant variations were observed along both the sidewall and inclined bed. Minimum boundary shear stress was observed at the corner and maximum skin friction occurred on the inclined bed, albeit the shear stress distribution was non-uniform in the transverse direction.

For all unsteady experiments, the positive surges were generated by the fast closure of the Tainter gate and the compression wave propagated upstream against the initially-steady flow. Figure 3 illustrate photographs of advancing bores. For the breaking surge experiments, the Tainter gate was

fully closed (h = 0). The surge strength, hence its Froude number, could be decreased by increasing the gate opening h after closure. The gate closure time was between 0.1 s and 0.2 s, small enough to have a negligible effect on the surge propagation. Table 1 summarises the experimental flow conditions.

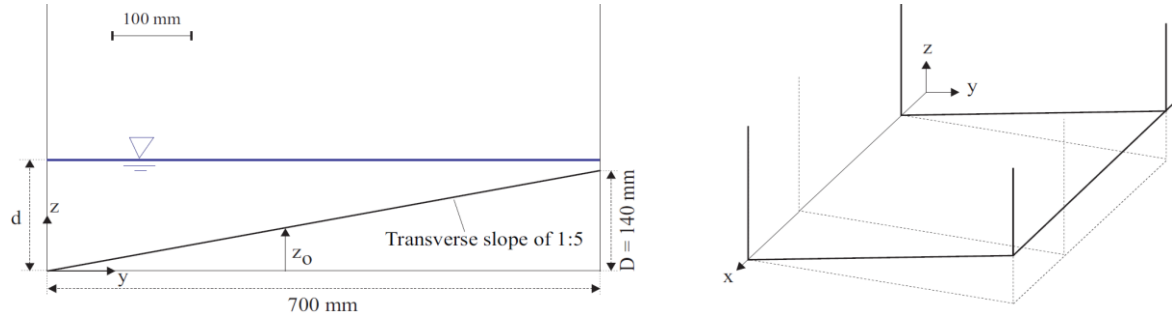

Figure 2 – Dimensioned sketch of the channel cross-section.

Table 1 – Experimental flow conditions

Run	Q (m^3/s)	S_o	d_1 (m)	h (m)	U (m/s)	Fr_1	Surge type
Steady flow	0.0147 to 0.1017	0.002216	0.10 to 0.21	N/A	N/A	N/A	N/A
Unsteady flow	0.100		0.207	0-0.067	0.2-1.1	1.3-1.8	Undular & Breaking
	0.055		0.167		0.67	1.53	
	0.030		0.130		0.4-0.6	1.11-1.15	

(A)

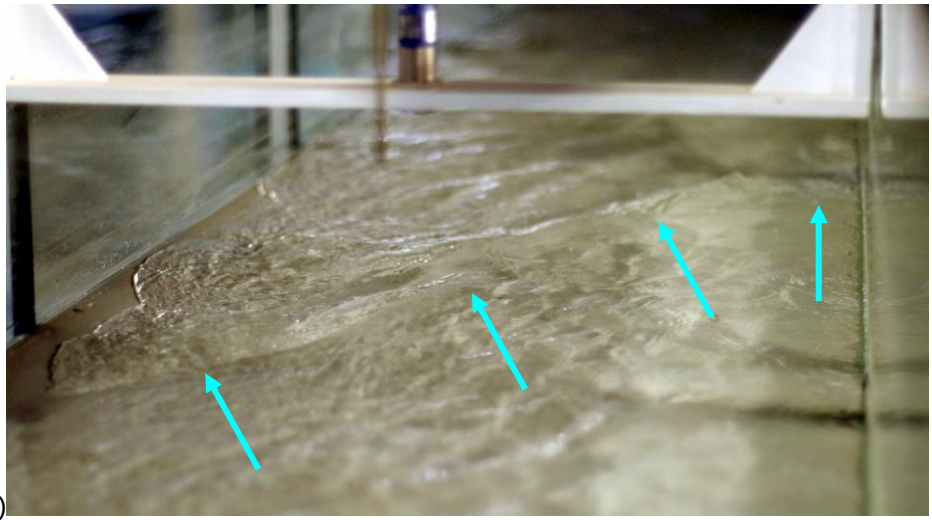

(B)

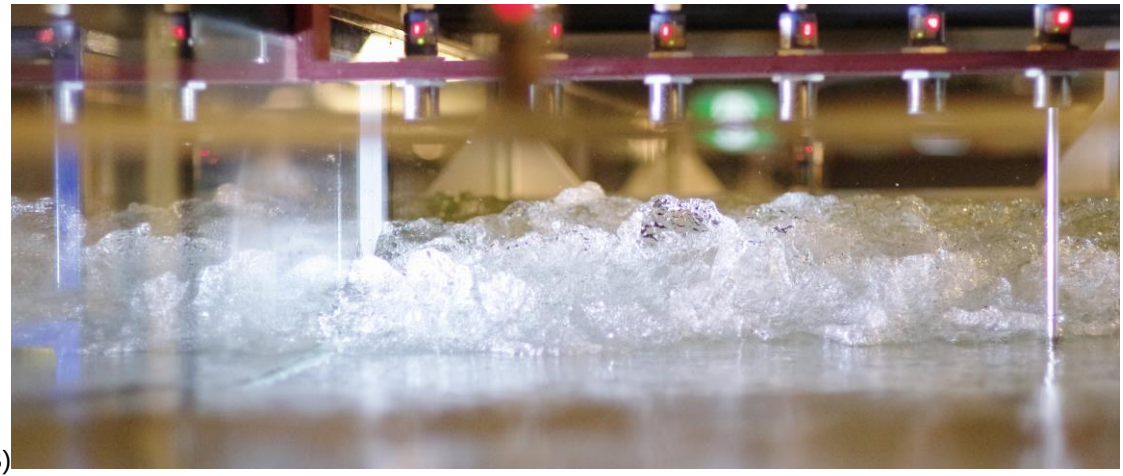

Figure 3 – Positive surge propagation in the experimental channel, looking downstream. (A) Three-dimensional surge: S_o = 0.002216, Q = 0.0314 m^3/s, Fr_1 = 1.1, d_1 = 0.130 m, h = 0.016 m, light blue arrows point to leading edge. (B) Breaking surge: S_o = 0.002216, Q = 0.10 m^3/s, Fr_1 = 1.6, d_1 = 0.2 m, h = 0 mm

3. UNSTEADY FLOW OBSERVATIONS

3.1. Presentation

In a non-rectangular channel, the upstream propagation of a positive surge may be analysed in an integral form (Cunge et al. 1980, Chanson 2012), albeit the classical Bélanger equation does not apply. Instead, a detailed solution for a irregular channel yields a theoretical solution between the ratio of conjugate to initial cross-section areas A_2/A_1 and the surge Froude number

$$Fr_1 = \frac{V_1 + U}{\sqrt{g \times \frac{A_1}{B_1}}} \quad (1)$$

where U the surge celerity positive upstream. For a smooth horizontal irregular channel, the exact solution is (Chanson 2012):

$$\frac{A_2}{A_1} = \frac{1}{2} \times \left(\sqrt{\left(2 - \frac{B'}{B}\right)^2 + 8 \times \frac{\frac{B'}{B}}{\frac{B_1}{B}} \times Fr_1^2} - \left(2 - \frac{B'}{B}\right) \right) \times \frac{B}{B'} \quad (2)$$

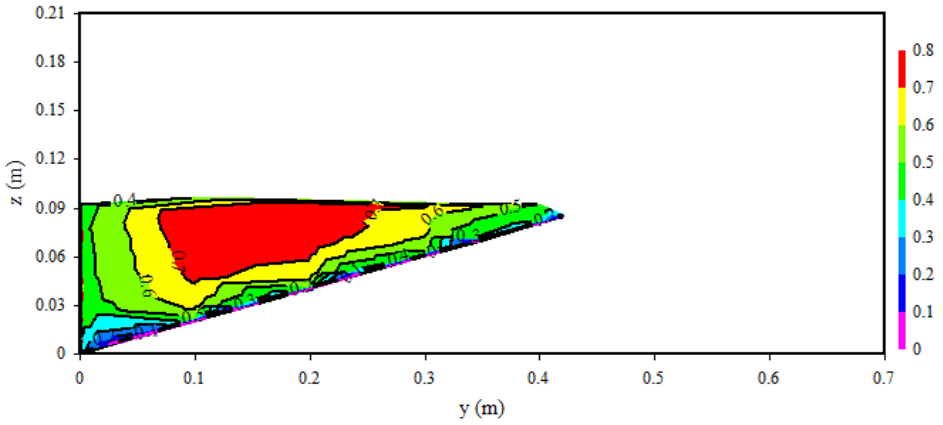

(A)

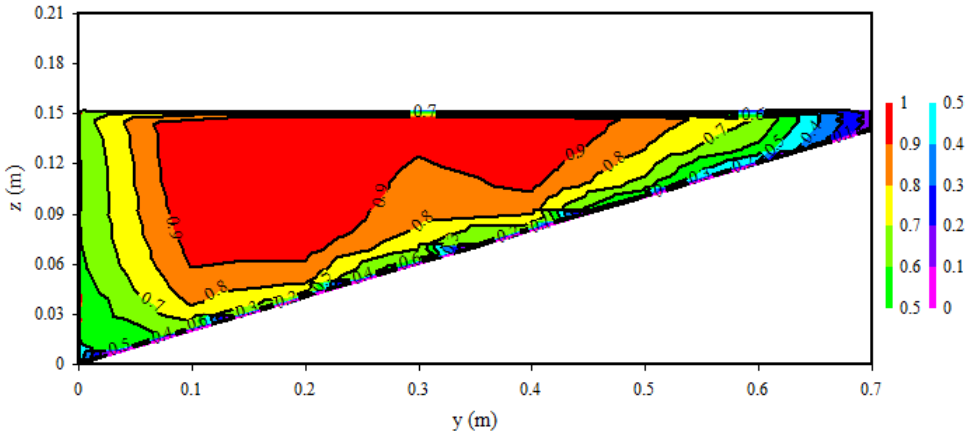

(B)

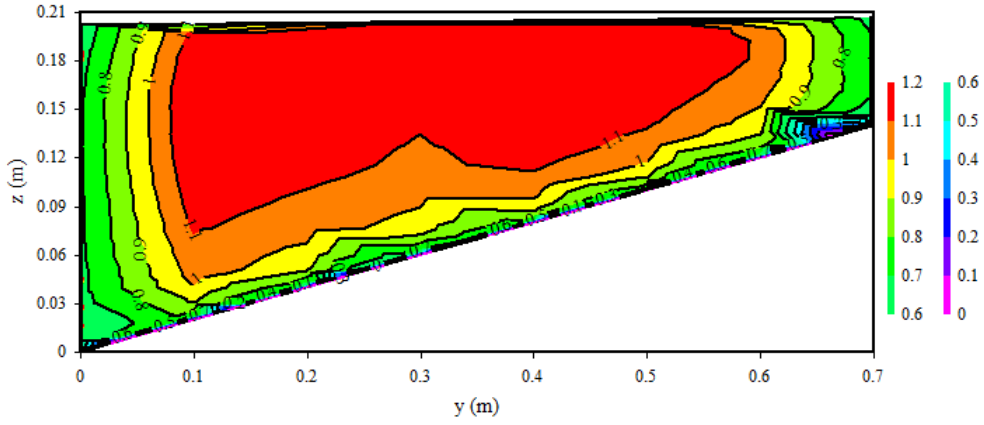

(C)

Figure 4 – Steady flow velocity contour plots in the trapezoidal channel (S_o = 0.002215957). (A) Q = 0.0147 m³/s. (B) Q = 0.050 m³/s. (C) Q = 0.1017 m³/s. Legend: velocity in m/s.

where the subscript 1 refers to the initial flow conditions, the subscript 2 corresponds to the conjugate flow conditions immediately behind the surge front, and B and B' are characteristic channel widths, defined as functions of the cross-section shape:

$$B = \frac{A_2 - A_1}{d_2 - d_1} \tag{3}$$

$$B' = \int_{A_1}^{A_2} (d_2 - z) \times dA \times \left(\frac{1}{2} \times (d_2 - d_1)^2 \right)^{-1} \quad (4)$$

3.2. Unsteady flow patterns

Visual observations were conducted for a range of initial flow conditions, in terms of discharge Q, and gate opening after closure h, with initial depths d_1, measured next to the right sidewall (i.e. measured above the lowest cross-sectional bed elevation), ranging from less than 0.1 m to more than 0.2 m. Figure 3 presents two photographs. For all sets of initial flow conditions, several main flow patterns were observed at the sampling site x = 8.6 m, depending upon the surge Froude number Fr_1 as well as the relative initial flow depth d_1/D, where D is the maximum height of the transverse bed slope: D = 0.140 m (Fig. 2). For $d_1/D < 1$, the initial free-surface width B_1 was less than 0.70 m and the initial cross-section area was triangular. Within the experimental flow conditions (Table 1), the surge rose past end of the transverse slope and the conjugate cross-section was trapezoidal, with a conjugate free-surface width B_2 = 0.70 m. Figure 3A shows such an experiment. For $d_1/D > 1$, both initial and conjugate free-surface widths were equal to 0.70 m and the corresponding flow cross-sections were trapezoidal.

For $Fr_1 > 1.5$ and the largest flow rate, the positive surge was breaking (Fig. 3B). The roller region was quasi-two-dimensional and air bubble entrainment was observed through the glass sidewalls in large-scale coherent structures. For all other flow conditions (Table 1), the surge was undular with some breaking, albeit with three-dimensional features. That is, the bore was undular in the deeper side, albeit some breaking was observed towards the left side where the water was shallower. The surge leading edge arrived first in the shallow water side and trailed in the deep water. That is, the surge propagated up the channel at an angle to the sidewall, although the bore celerity was the same on both sides of the flume. Some complicated three-dimensional flow motion was observed behind the bore front, with transient secondary currents in the wake of the shallow-water bore front.

For $d_1/D < 1$, visual observations highlighted characteristic three-dimensional features, with strong transverse mixing illustrated by large-scale vortices and surface scars behind the surge front. Dye injection showed drastically different conjugate motions between the left and right sides. In the deeper side (right), the conjugate flow motion continued to flow downstream, while, in the shallower (left) side, the flow changed direction after the bore, moving upstream. This led to some complicated secondary currents and shear zone about the channel centreline.

Overall the current findings presented some similarity with positive surge propagation in a compound channel (Pan and Chanson 2015), and with field observations of tidal bore in trapezoidal channels, e.g. Garonne River at Arcins (Chanson et al. 2010, Keevil et al. 2015, Reungoat et al. 2017).

3.3. Unsteady flow field

The positive surge was generated at the downstream end of the channel immediately after the rapid gate closure. As the water piled up against the gate, the bore formed and propagated upstream, its shape evolving in response to the asymmetrical channel shape. While the surge shape evolved rapidly during the initial instants, its shape varied more gradually for x < 12-14 m. At the sampling point x = 8.6 m, the free-surface elevation rose rapidly during the surge passage.

Instantaneous free-surface elevation and velocity measurements were conducted continuously at high frequency (100 Hz). Figure 5 shows a typical data set for a breaking bore with undulations and $d_1/D > 1$, in terms of the surface elevation z and longitudinal velocity component V_x, positive downstream, at several transverse locations y. In Figure 5, the data were ensemble-averaged and $z-z_o$ is the local elevation above the bed. The free-surface data showed that the surge was three-dimensional (Fig. 5A). That is, it was breaking in the shallow water side and undular in the deep-water side. Prior to the surge passage, the current velocity was positive downstream. The surge passage had a marked effect on the velocity field, as seen in Figure 5B. This included a rapid flow deceleration and large and rapid fluctuations of all velocity components behind the surge front. The present observations were consistent with earlier observations in rectangular channels (Koch and Chanson 2009, Chanson 2010, Leng and Chanson 2016), albeit a key feature was the three-dimensional nature of the surge front.

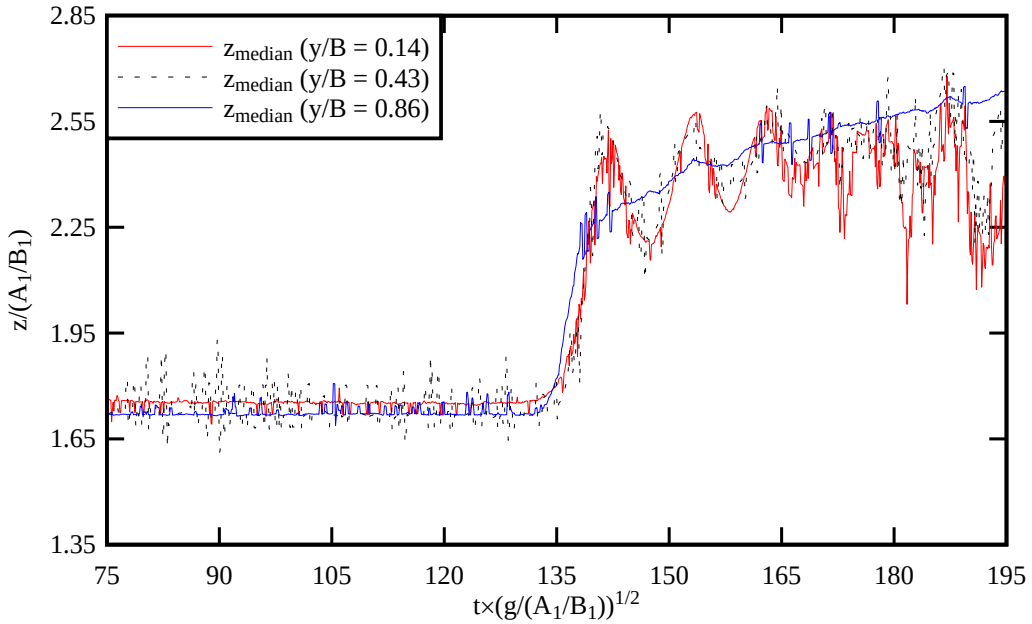

(A)

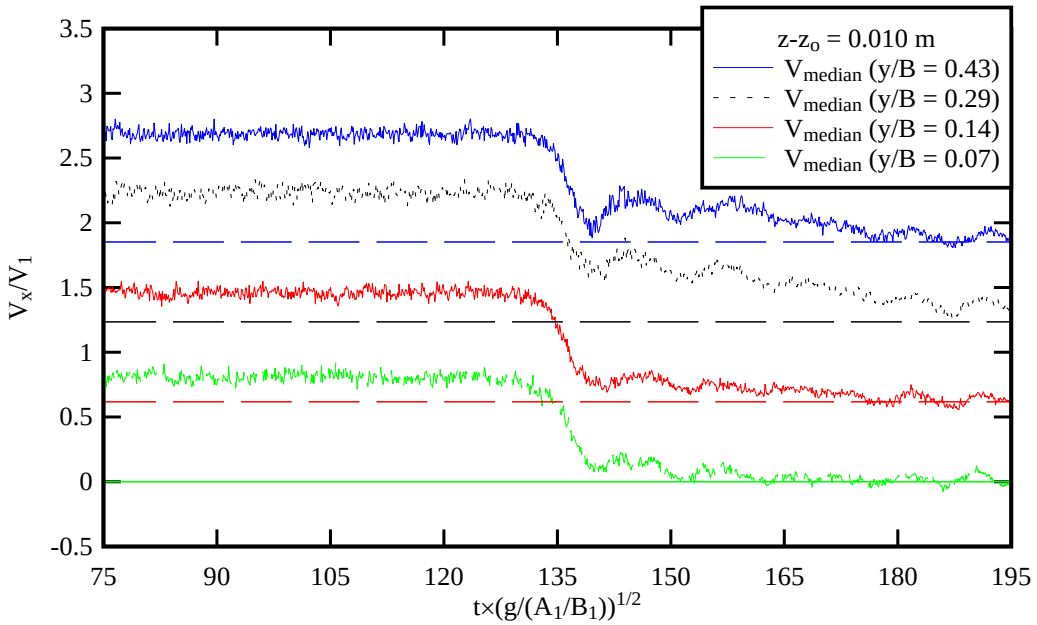

(B)

Figure 5 – Dimensionless time-variations of unsteady water elevation and longitudinal velocity component during positive surge propagation in the trapezoidal channel. Flow conditions: S_o = 0.002216, Q = 0.055 m^3/s, d_1 = 0.167 m, U = 0.67 m/s, Fr_1 = 1.53, ensemble-median data. (A) Water elevations at three transverse locations. (B) Longitudinal velocity at $z-z_o$ = 0.010 m at four transverse locations; data shifted upwards by 0.62 between two adjacent curves.

4. CONCLUSION

A laboratory investigation of positive surges in an asymmetrical trapezoidal channel was conducted in a large-size facility (19 m long, 0.7 m wide). Detailed measurements were conducted at relatively high-frequency using several acoustic displacement meters and an acoustic Doppler velocimeter profiler. The study focused on the unsteady turbulent properties.

The surge flow was a function of both the Froude number Fr_1 and relative initial flow depth d_1/D. The free-surface data presented markedly three-dimensional flow features. The velocity measurements showed a drastic impact of the surge on the flow field, showing strong three-dimensional features in

the asymmetrical channel. The surge passage induced a rapid flow deceleration and large and rapid fluctuations of all velocity components behind the surge front. While the present observations presented some similarity to earlier observations in rectangular channels, a key feature was the three-dimensional nature of the surge front in the asymmetrical trapezoidal channel. The experimental results showed a transient three-dimensional surge flow associated with some transverse mixing induced by unsteady secondary motion.

Overall the unsteady turbulent field presented marked differences compared to observations in rectangular channels. The findings may be directly relevant to surge propagation in man-made trapezoidal waterways and natural irregular-shaped channels in terms of numerical modelling. Classical depth-averaged numerical models, e.g. based upon St Venant equations, Boussinesq equations, are inappropriate to model the complicated three-dimensional turbulent mixing beneath surges in irregular channels. A full three-dimensional computational fluid dynamics (3D CFD) model based upon the Navier-stokes equations is required, albeit a proper validation is critical and necessitates suitable physical modelling data (Leng et al. 2017, Lubin and Chanson 2017).

5. ACKNOWLEDGMENTS

The authors acknowledge the assistance of Pedro Xavier Sanchez Michilena and Ruben Eduardo Freire Quillupangui with experimental measurements. The technical support of Jason Van Der Gevel and Steward Matthews is acknowledged. The financial support of the Australian Research Council (ARC DP120100481) and of the School of Civil Engineering, the University of Queensland is acknowledged. Helpful discussions with Prof. Pierre Lubin are acknowledged.

6. REFERENCES

Benet, F., and Cunge, J.A. (1971). *Analysis of Experiments on Secondary Undulations caused by Surge Waves in Trapezoidal Channels*. Journal of Hydraulic Research, IAHR, Vol. 9, No. 1, pp. 11-33.

Cabonce, J., Fernando, R., Wang, H., and Chanson, H. (2017). *Using Triangular Baffles to Facilitate Upstream Fish Passage in Box Culverts: Physical Modelling*. Hydraulic Model Report No. CH107/17, School of Civil Engineering, The University of Queensland, Brisbane, Australia.

Chanson, H. (2004). *The Hydraulics of Open Channel Flow: An Introduction*. Butterworth-Heinemann, 2nd edition, Oxford, UK, 630 pages.

Chanson, H. (2010). *Unsteady Turbulence in Tidal Bores: Effects of Bed Roughness*. Journal of Waterway, Port, Coastal, and Ocean Engineering, ASCE, Vol. 136, No. 5, pp. 247-256 (DOI: 10.1061/(ASCE)WW.1943-5460.0000048).

Chanson, H. (2011). *Tidal Bores, Aegir, Eagre, Mascaret, Pororoca: Theory and Observations*. World Scientific, Singapore, 220 pages.

Chanson, H. (2012). *Momentum Considerations in Hydraulic Jumps and Bores*. Journal of Irrigation and Drainage Engineering, ASCE, Vol. 138, No. 4, pp. 382-385 (DOI 10.1061/(ASCE)IR.1943-4774.0000409).

Chanson, H., Reungoat, D., Simon, B., and Lubin, P. (2011). *High-Frequency Turbulence and Suspended Sediment Concentration Measurements in the Garonne River Tidal Bore*. Estuarine Coastal and Shelf Science, Vol. 95, No. 2-3, pp. 298-306 (DOI 10.1016/j.ecss.2011.09.012).

Cunge, J.A. (1975). *Rapidly Varying Flow in Power and Pumping Canals*. In *Unsteady Flow in Open Channels*. WRP Publ., Fort Collins, USA, K. Mahmood and V. Yevdjevich Ed., Vol. 2, pp. 539-586.

Cunge, J.A., Holly Jr, F.M., and Verwey, A. (1980). *Practical Aspects of Computational River Hydraulics*. Pitman, Boston, USA, 420 pages.

Furgerot, L., Mouaze, D., Tessier, B., Perez, L., Haquin, S., Weill, P., and Crave, A. (2016). *Sediment transport induced by tidal bores. An estimation from suspended matter measurements in the Sée River (Mont-Saint-Michel Bay, northwestern France)*. Comptes Rendus Géoscience, Vol. 348, pp. 432-441 (DOI: 10.1016/j.crte.2015.09.004).

Henderson, F.M. (1966). *Open Channel Flow*. MacMillan Company, New York, USA.

Keevil, C.E., Chanson, H., and Reungoat, D. (2015). *Fluid Flow and Sediment Entrainment in the Garonne River Bore and Tidal Bore Collision*. Earth Surface Processes and Landforms, Vol. 40, No. 12, pp. 1574-1586 (DOI: 10.1002/esp.3735).

Koch, C., and Chanson, H. (2009). *Turbulence Measurements in Positive Surges and Bores*. Journal of Hydraulic Research, IAHR, Vol. 47, No. 1, pp. 29-40 (DOI: 10.3826/jhr.2009.2954)

Leng, X., and Chanson, H. (2016). *Coupling between Free-surface Fluctuations, Velocity Fluctuations and Turbulent Reynolds Stresses during the Upstream Propagation of Positive Surges, Bores and Compression Waves*. Environmental Fluid Mechanics, Vol. 16, No. 4, pp. 695-719 & digital appendix (DOI: 10.1007/s10652-015-9438-8).

Leng, X., and Chanson, H. (2017). *Upstream Propagation of Surges and Bores: Free-Surface Observations*. Coastal Engineering Journal, Vol. 59, No. 1, paper 1750003, 32 pages & 4 videos (DOI: 10.1142/S0578563417500036).

Leng, X., Lubin, P., and Chanson, H. (2017). *CFD Modelling of Breaking and Undular Tidal Bores with Physical Validation*. Proceedings of 37th IAHR World Congress, IAHR & USAINS Holding Sdn. Bhd. Publ., Editors Aminuddin Ab. Ghani, Ngai Weng Chan, Junaidah Ariffin, Ahmad Khairi Abd Wahab, Sobri Harun, Amir Hashim Mohamad Kassim and Othman Karim, Kuala Lumpur, Malaysia, 13-18 August, Vol. 7, Theme 7.1, pp. 5072-5081.

Lubin, P., and Chanson, H. (2017). *Are breaking waves, bores, surges and jumps the same flow?* Environmental Fluid Mechanics, Vol. 17, No. 1, pp. 47-77 (DOI: 10.1007/s10652-016-9475-y).

Pan, D.Z., and Chanson, H. (2015). *Physical Modelling of Tidal Bore Dyke Overtopping: Implication on Individuals' Safety*. Proc. 36th IAHR World Congress, The Hague, The Netherlands, 27 June-3 July, Theme 4, pp. 3824-3831,

Ponsy, J., and Carbonnell, M. (1966). *Etude Photogrammétrique d'Intumescences dans le Canal de l'Usine d'Oraison (Basses-Alpes)*. Journal de la Société Française de Photogram., Vol. 22, pp. 18-28.

Sandover, J.A., and Taylor, C. (1962). *Cnoidal waves and bores*. Journal La Houille Blanche, No. 3, Sept., pp. 443-445.

Treske, A. (1994). *Undular Bores (Favre-Waves) in Open Channels - Experimental Studies*. Journal of Hydraulic Research, IAHR, Vol. 32, No. 3, pp. 355-370.

Yasuda, H. (2010). *One-Dimensional Study on Propagation of Tsunami Wave in River Channels*. Journal of Hydraulic Engineering, ASCE, Vol. 136, No. 2, pp. 93-105.